

# Asymmetric cell division in fucoid algae: a role for cortical adhesions in alignment of the mitotic apparatus

Sherryl R. Bisgrove and Darryl L. Kropf

University of Utah, Department of Biology, 257 South 1400 East, Salt Lake City, UT 84112-0840, USA

Author for correspondence (e-mail: bisgrove@biology.utah.edu)

Accepted 11 August 2001

Journal of Cell Science 114, 4319-4328 (2001) © The Company of Biologists Ltd

## SUMMARY

The first cell division in zygotes of the fucoid brown alga *Pelvetia compressa* is asymmetric and we are interested in the mechanism controlling the alignment of this division. Since the division plane bisects the mitotic apparatus, we investigated the timing and mechanism of spindle alignments. Centrosomes, which give rise to spindle poles, aligned with the growth axis in two phases – a premetaphase rotation of the nucleus and centrosomes followed by a postmetaphase alignment that coincided with the separation of the mitotic spindle poles during anaphase and telophase. The roles of the cytoskeleton and cell cortex

in the two phases of alignment were analyzed by treatment with pharmacological agents. Treatments that disrupted cytoskeleton or perturbed cortical adhesions inhibited premetaphase alignment and we propose that this rotational alignment is effected by microtubules anchored at cortical adhesion sites. Postmetaphase alignment was not affected by any of the treatments tested, and may be dependent on asymmetric cell morphology.

Key words: Adhesions, Asymmetric cell division, Brown algae, Spindle alignment

## INTRODUCTION

Controlling the positions of cell divisions is one of the primary mechanisms for regulating sizes, shapes, fates and spatial relationships among cells in a developing organism. Asymmetric cell divisions, in particular, play important roles in development. An asymmetric division produces two cell types that differ in size, morphology, and/or the developmental determinants that they inherit. In the latter case, determinants are polarized within a cell and the division plane partitions these determinants unequally between the daughter cells, producing two cells with different developmental fates. Such asymmetric divisions occur during development in many organisms including *Caenorhabditis elegans* and *Drosophila melanogaster* (Hawkins and Garriga, 1998; Rose and Kemphues, 1998). Asymmetric divisions often produce daughter cells of different sizes or morphologies. The green alga *Volvox carteri*, for example, undergoes a series of asymmetric cell divisions that produce two cell types, small somatic cells and larger reproductive gonidial cells, and it is the size of the cell that determines its fate (Kirk et al., 1993). The first embryonic division in fucoid brown algae also produces daughter cells that differ in size and morphology, and the proper placement of this asymmetric division is important for subsequent embryonic growth (Bisgrove and Kropf, 1998). This report concerns the mechanism by which this division is positioned.

The mechanisms by which cells position division planes during asymmetric divisions are currently under investigation in several model organisms. In many of these organisms genetic analyses are providing new insights into the genes that

regulate division plane alignments but cellular and physiological analyses are often impeded because the relevant cells are small in size or inaccessible. By contrast, zygotes of fucoid algae are amenable to cellular and physiological manipulations and therefore provide a complementary model system in which to analyze the mechanism of division plane alignment. The major advantages are that (1) eggs and sperm are released into the surrounding seawater and can be easily harvested in large numbers, (2) eggs and zygotes are large cells, approximately 100 µm in diameter, facilitating physiological studies, and (3) populations of zygotes develop synchronously, free of maternal influences, which allows analyses to be easily targeted to specific stages of development (Kropf, 1997; Fowler and Quatrano, 1997; Kropf et al., 1999).

The first zygotic division in fucoid algae is an asymmetric division in which the mitotic apparatus aligns parallel with the growth axis and cytokinesis bisects the mitotic apparatus, thereby ensuring that the nascent crosswall is transverse to the growth axis. We have speculated that alignment of the mitotic apparatus occurs by a rotational mechanism in which microtubules anchored to cortical adhesions provide the requisite force (Kropf, 1997). Sites of tight adhesion of plasma membrane to cell wall (cortical adhesions) can be visualized by plasmolyzing germinated zygotes using hypotonic solutions, and these adhesions contain F-actin on their cytosolic face (Henry et al., 1996). Adhesions have also been observed in other walled cells including those of angiosperms (Kohorn, 2000), ferns (Kagawa et al., 1992), and fungi (Kaminskyj and Heath, 1995), but their molecular nature and functions are largely unknown (Kohorn, 2000). It has been postulated that adhesions may be involved in plant responses

to fungal infection (Mellersh and Heath, 2001), defining cortical division sites (Cleary, 2001), directing cell expansion (Kaminskyj and Heath, 1995; Bachewich and Heath, 1997; Kohorn, 2000), maintaining cellular polarity (Fowler and Quatrano, 1997; Kropf et al., 1999), facilitating cytoplasmic movements (Bachewich and Heath, 1997), and positioning nuclei and/or other organelles within cells (Kropf, 1997).

We have investigated the timing of the alignment process and tested the hypothesis that cytoskeleton and cortical adhesions function in aligning the mitotic apparatus during asymmetric cell division in fucoid algae. We report that alignment occurs in two phases – a premetaphase rotation of the nucleus followed by a postmetaphase alignment that coincides with the separation of the mitotic spindle poles. Interestingly, disruption of cytoskeleton or cortical adhesions specifically inhibits the premetaphase rotational alignment, providing evidence that the cytoskeleton interacts with cortical adhesions to position the nucleus during asymmetric division.

## MATERIALS AND METHODS

### Culture

Sexually mature receptacles of the fucoid alga *Pelvetia compressa* (J. Agardh) *De Toni* [proposed renaming to *Silvetia compressa* (Serrao et al., 1999)] were collected near Santa Cruz, CA, shipped cold and stored at 4°C until use. To induce the release of zygotes, receptacles were placed in the light (100  $\mu\text{mol photons/m}^2/\text{s}$ ) at 16°C in artificial sea water (ASW; 10 mM KCl, 0.45 M NaCl, 9 mM  $\text{CaCl}_2$ , 16 mM  $\text{MgSO}_4$  and 0.040 mg/ml chloramphenicol, buffered to pH 8.2 with 10 mM Tris base) overnight and then transferred to the dark for 30–45 minutes. The time of fertilization was considered to be the midpoint of the dark period. All zygotes were grown at 16°C in unidirectional light.

### Inhibitor treatments and removal of sulfate

Generally, treatments were initiated after germination and were chronic. Exceptions to this general protocol were as follows: olomoucine was added 5 hours after fertilization [AF; during S phase of the cell cycle (Corellou et al., 2000)] and olomoucine-containing solutions were replaced every 12 hours; isoxaben was added and/or sulfate was removed within 1 hour AF.

All pharmacological agents were diluted to the appropriate concentrations in ASW from stock solutions that were made as follows: olomoucine (a gift from Francois-Yves Bouget, CNRS, Roscoff, France), 0.1 M in dimethyl sulfoxide (DMSO); isoxaben (a gift from I. Larrinua, Dow AgroSciences Discovery Research, Indianapolis), 0.1 M in DMSO; latrunculin B, 50  $\mu\text{M}$  in DMSO; Brefeldin A, 2.5 mg/ml in ethanol; oryzalin, 10 mM in DMSO; paclitaxel, 10 mM in DMSO. Sucrose, sorbitol, thermolysin and proteinase K were all dissolved directly in ASW. The sulfate was lowered by rinsing zygotes 8–10 times (5 minutes each) in ASW without  $\text{MgSO}_4$  (low sulfate ASW).

### Immunofluorescence microscopy

Coverslips with attached *P. compressa* zygotes were frozen for 1–2 seconds in liquid nitrogen and thawed into fixative containing 3% paraformaldehyde, 0.5% glutaraldehyde in PHEM buffer (60 mM Pipes, 25 mM Hepes, 10 mM EGTA, 2 mM  $\text{MgCl}_2$ , pH 7.5) with 4% NaCl. After a 1–2 hours fixation coverslips were immersed again (1–2 seconds) in liquid nitrogen, thawed in fixative, and then rinsed with modified PBS (mPBS; 137 mM NaCl, 2.7 mM KCl, 1.7 mM,  $\text{KH}_2\text{PO}_4$ , 5% glycerol, 0.1% sodium azide, 0.1% bovine serum albumin (BSA)). Unless otherwise noted, all of the following incubations and rinses were carried out at room temperature and all

rinses were repeated three times, for 5 minutes each. Zygotes were incubated overnight in mPBS with 5% Triton X-100 added to extract pigments, rinsed with mPBS, and incubated overnight in mPBS containing 100 mM  $\text{NaBH}_4$ . The  $\text{NaBH}_4$  incubation was followed with mPBS rinses, a single rinse in C medium (100 mM NaCl, 20 mM  $\text{MgCl}_2$ , 2 mM KCl, 0.2% BSA, 10 mM MES, 0.85 M sorbitol, 1 mM EGTA, with pH adjusted to 5.8 with Tris base), and a 30 minute incubation in C medium with cell wall degrading enzymes (7 mg/ml cellulase (CELFL, Worthington Biochemical Corp., Freehold NJ), 40 mg/ml hemicellulase, 7 mg/ml abalone gut extract, 0.1 mM phenylmethyl sulfonyl fluoride). Following wall digestion, zygotes were rinsed once with C medium and then with mPBS. Samples were blocked overnight in 2.5% w/v nonfat dry milk in mPBS, rinsed with mPBS, and incubated overnight with monoclonal anti- $\alpha$ -tubulin antibodies (DM1A; Sigma) diluted 1:50 in mPBS. Zygotes were rinsed in mPBS, incubated overnight in rhodamine-conjugated goat anti-mouse IgG (Cappel™, Durham NC) diluted 1:50 in mPBS, rinsed again in mPBS, extracted with 100% methanol (three rinses, 10 minutes each) and mounted in clearing solution (2:1 benzyl benzoate:benzyl alcohol). Fluorescence images were obtained on either a MRC-600 (Bio-Rad Laboratories, Richmond, CA) or a LSM510 (Carl Zeiss Inc., Thornwood, NY) laser-scanning confocal microscope using, respectively, a 568 or a 543 nm laser line with 578–618 or 560–600 nm narrow band pass emission filter.

The centrosomal alignment angle, defined as the angle between the rhizoid/thallus growth axis and a line drawn through the two centrosomes, was measured on zygotes labeled with anti- $\alpha$ -tubulin antibodies using a protractor in the eyepiece of an Olympus inverted microscope. The distances separating the two centrosomes were measured on images captured with a cooled CCD camera (CoolSNAP™, Roper Scientific, Tucson AZ) mounted on the same microscope. Cell plate alignments were measured on living zygotes either unstained or stained with 5  $\mu\text{M}$  FM® 4-64 (Molecular Probes Inc., Eugene OR) diluted from a 20 mM DMSO stock. Statistical analyses were performed with either a parametric or a nonparametric *t*-test, as appropriate.

## RESULTS

### Timing of centrosomal alignment

The angle between the centrosomal axis and the growth axis (alignment angle) was measured on zygotes from several populations that had been labeled with anti- $\alpha$ -tubulin antibodies. Developmental stage was assayed as the percent of zygotes at or past metaphase. When populations were sampled early in the progression into mitosis (15% or fewer zygotes had progressed into or past metaphase), the mean alignment angle in premetaphase zygotes was approximately 45° (Fig. 1A). Alignment angles were distributed approximately equally between 0 and 90° (Fig. 1B), indicating that the centrosomal axes were randomly positioned with respect to the growth axes. As a population transitioned through mitosis, alignment angles in premetaphase zygotes decreased indicating that some alignment of the centrosomal axes occurred prior to entry into metaphase. The extent of alignment that occurred prior to spindle formation varied between populations. In some populations alignment improved by only a few degrees prior to spindle formation (Fig. 1A, gray diamonds); in other populations close to 20° of premetaphase alignment occurred (Fig. 1A, gray circles; in linear regression analysis  $y = -0.36x + 45$ ,  $R^2 = 0.98$ ). Although alignment angles in metaphase were widely distributed, they were skewed toward 0° (Fig. 1B). Little to no alignment occurred during metaphase (Fig. 1A),

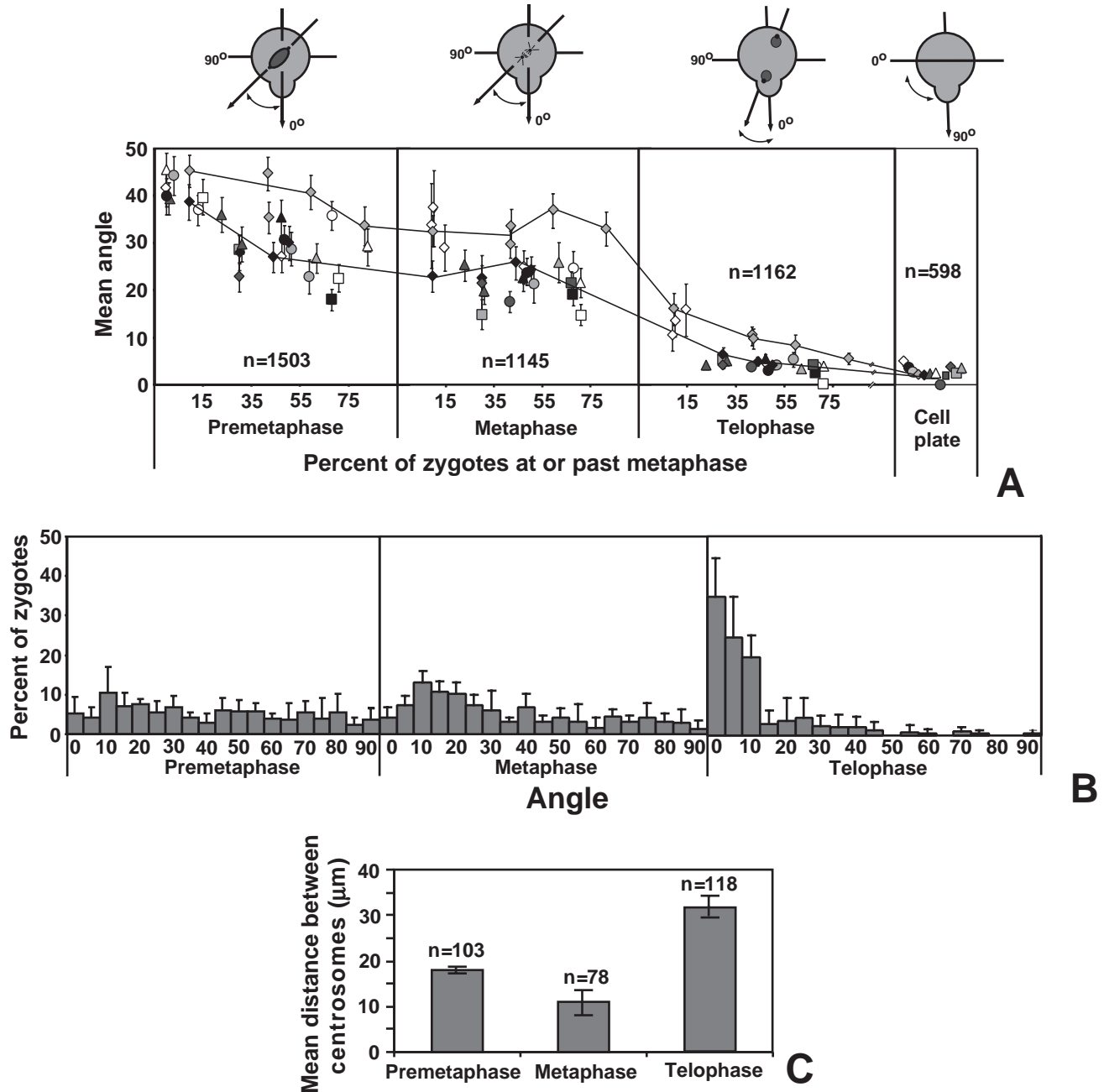


**Fig. 1.** Centrosomal alignment (A,B) and distances between the centrosomes (C) in zygotes progressing into and through mitosis. (A) Fifteen populations were developmentally staged by assaying the percent of zygotes at or past metaphase; the alignment angles were measured on zygotes stained with anti- $\alpha$ -tubulin antibodies and the angle between the cell plate and the growth axis was measured on living embryos stained with FM® 4-64. Each symbol designates a different population and data points are the mean angles  $\pm$  s.e.m. in each population. (B) Distribution of alignment angles in one population of zygotes (A, grey circles). Each bar represents the mean from three timepoints  $\pm$  s.d. (C) Distances between centrosomes; bars indicate the mean of three populations  $\pm$  s.d.

but alignment resumed after metaphase. Few zygotes were observed in anaphase, indicating that this stage of mitosis was short; no measurements were made on anaphase arrays. Nonetheless, considerable alignment probably occurred during anaphase since alignments in early telophase were better than metaphase alignments (Fig. 1A). By late telophase, alignment angles were tightly grouped between  $0^\circ$  and  $10^\circ$  (Fig. 1B), and were as well aligned as the cell plates that subsequently formed (Fig. 1A). These data suggest that the alignment process occurs

in two phases, a premetaphase rotational alignment of the nucleus and centrosomes and a postmetaphase alignment during anaphase and telophase.

As zygotes progressed into and through mitosis, the distance between the two centrosomes also changed (Fig. 1C). Prior to metaphase the centrosomes were on opposite sides of the nucleus and  $18 \pm 0.75 \mu\text{m}$  apart. During metaphase spindle poles were only  $11 \pm 2.6 \mu\text{m}$  apart, but afterwards the mitotic apparatus elongated nearly threefold resulting in centrosomes

on daughter nuclei being  $32 \pm 2.5$   $\mu\text{m}$  apart in late telophase. Elongation of the centrosomal axis, therefore, correlated temporally with postmetaphase alignment.

### Microtubules

Representative confocal images of centrosomes and microtubules are shown in Fig. 2. In optical sections near the midplane of premetaphase zygotes, microtubules extended from the perinuclear centrosomes out to the cell cortex (Fig. 2A,B). The microtubules that emanated into the rhizoid appeared to be more densely packed than the microtubules that extended into the thallus. In some premetaphase zygotes the nucleus appeared nearly spherical (Fig. 2A), while in others the nucleus had elongated along the centrosomal axis and was more oval in shape (Fig. 2B). Usually the better aligned nuclei were more oval. Confocal images of the cortex in premetaphase zygotes revealed astral microtubules that bent and ran laterally in the cell cortex, within 1.5  $\mu\text{m}$  of the plasma membrane, as well as microtubules that appeared to terminate at right angles to the surface (Fig. 2E). When zygotes entered metaphase, however, microtubules disappeared from the cell cortex and astral microtubules were short (Fig. 2C,F). An extensive cytoplasmic microtubule array reappeared following metaphase; by telophase microtubules were again observed extending from the centrosomes to the cell periphery (Fig. 2D) where they either terminated perpendicular to the surface or curved and extended for some distance beneath the plasma membrane (Fig. 2G). These findings suggest that microtubule connections from nucleus to cortex may function in both phases of alignment.

To test the role of microtubules in each stage of alignment, zygotes in premetaphase were treated with low doses of paclitaxel or oryzalin to partially stabilize or partially depolymerize microtubules, respectively, and alignments were measured as zygotes progressed through mitosis. [More severe microtubule disruption blocked mitosis (Corellou et al., 2000).] Metaphase spindle alignments were significantly different than controls following oryzalin or paclitaxel treatment ( $P < 0.004$  for 0.1  $\mu\text{M}$  oryzalin;  $P < 0.0004$  for 0.3  $\mu\text{M}$  oryzalin;  $P < 0.002$  for 1  $\mu\text{M}$  paclitaxel), indicating that premetaphase alignment was disrupted (Fig. 3A). By contrast, postmetaphase alignment progressed normally in treated zygotes; alignment improved by approximately  $22^\circ$  in controls,  $24^\circ$  in 0.1  $\mu\text{M}$  oryzalin,  $22^\circ$  in 0.3  $\mu\text{M}$  oryzalin and  $29^\circ$  in 1  $\mu\text{M}$  paclitaxel. Separation of spindle poles also proceeded in treated zygotes (Fig. 3B), indicating that microtubules were still partially functional. Fewer microtubules were present in oryzalin and metaphase spindles lacked all astral microtubules (Fig. 3C,D). In paclitaxel, most zygotes had brightly staining foci, probably cytoplasmic asters (Fig. 3E), and did not develop. Measurements were taken on treated zygotes that continued development; these zygotes had less severely affected arrays with more cortical microtubules and occasionally cytoplasmic asters (Fig. 3F). Treatment with diclobenil also perturbed microtubular arrays (Bisgrove and Kropf, 2001) and prevented premetaphase, but not postmetaphase, alignment (data not shown).

### Adhesions

Cortical adhesions form a subapical ring in the rhizoid of germinated zygotes and have been postulated to play a role in

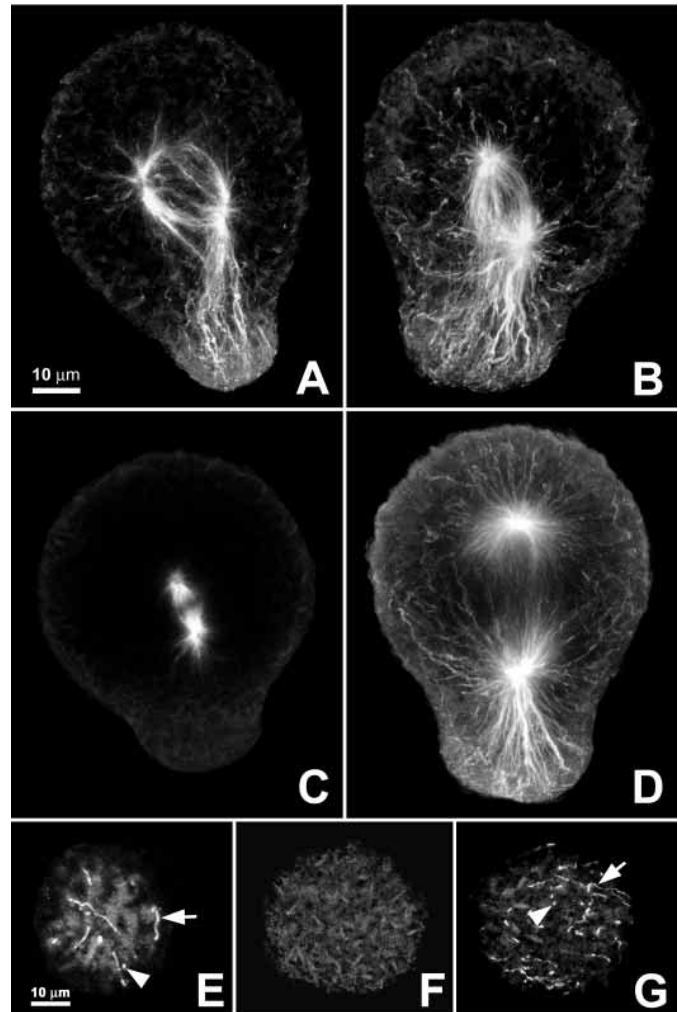


**Fig. 2.** Microtubule arrays during centrosomal alignment. (A-D) A projection of confocal sections representing a section 10–20  $\mu\text{m}$  thick in the midplane of zygotes. The zygotes are positioned with rhizoids towards the bottom of the page. (A,B) Prior to spindle formation, microtubules extended from the centrosomes to the cell cortex, and were concentrated in the rhizoid. (C) Metaphase spindles had short astral microtubules. (D) At telophase, microtubules again reached the cell cortices at both rhizoid and thallus poles. (E–G) Projections of confocal images from the outermost 1.5  $\mu\text{m}$  of the thallus cortex in premetaphase (E), metaphase (F) and telophase (G). Arrows indicate cortical microtubules parallel to, and just beneath, the plasma membrane and arrowheads indicate microtubules that terminate at right angles to the surface. Scale bar in A also applies to B–D; scale bar in E also applies to F and G.

centrosomal alignment (Henry et al., 1996; Kropf et al., 1999). To test this hypothesis, the effects of several treatments aimed at disrupting adhesions were examined at each phase of alignment.

### F-actin disruption

Cortical F-actin is present in subapical adhesions in rhizoids and F-actin depolymerization disrupts these adhesions (Henry et al., 1996). We investigated the requirement for F-actin in pre- and postmetaphase alignment using latrunculin B (Alessa and Kropf, 1999). Germinated zygotes were treated with

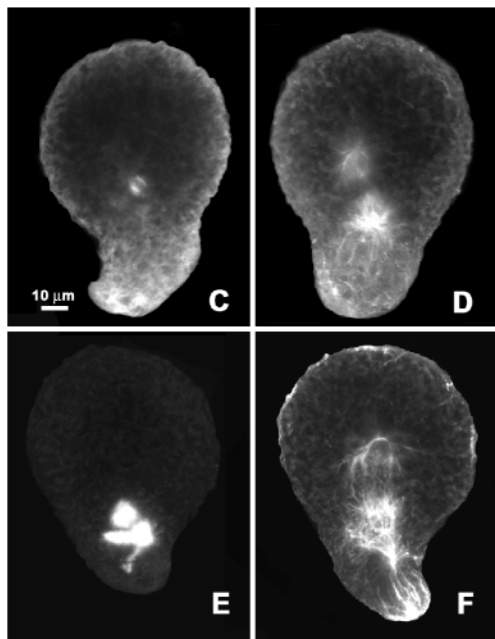
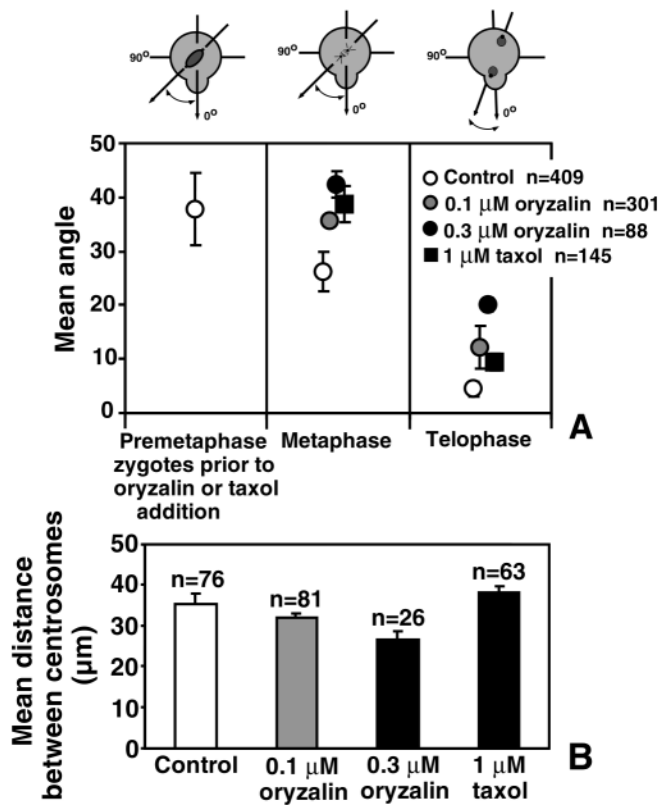


**Fig. 3.** Effects of low concentrations of oryzalin (0.1 or 0.3  $\mu\text{M}$ ) or paclitaxel (1  $\mu\text{M}$ ). Treatments were initiated 16–17 hours AF. (A) Centrosomal alignment angles were measured on zygotes prior to treatment and during mitosis. (B) Distances between centrosomes at telophase. Data points in A and bars in B are the means  $\pm$  s.d. of two or three experiments. (C–F) Microtubule arrays in 0.3  $\mu\text{M}$  oryzalin (C), 0.1  $\mu\text{M}$  oryzalin (D), or 1  $\mu\text{M}$  paclitaxel (E, F).

latrunculin B and centrosomal alignments were measured. Premetaphase alignment of the nucleus was inhibited in treated zygotes, resulting in metaphase alignments that were

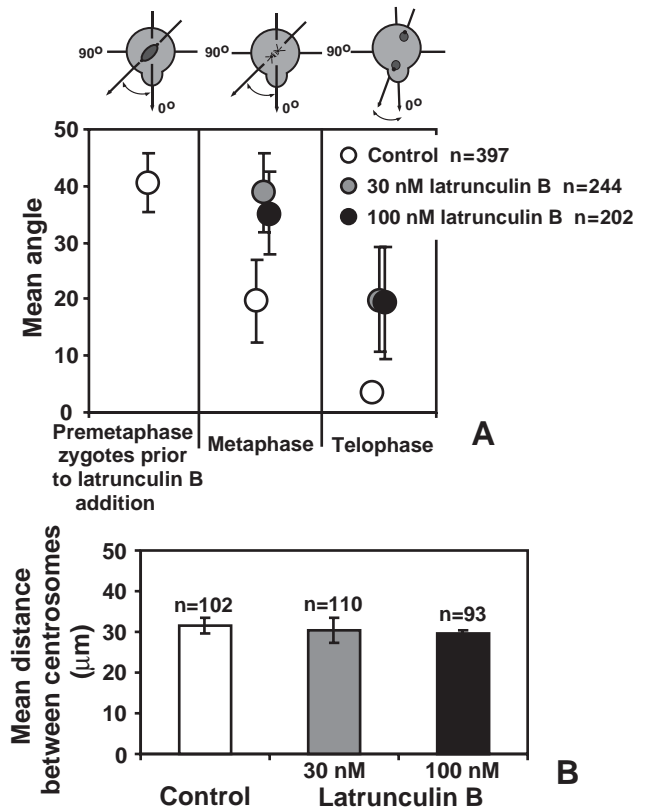


**Fig. 4.** Centrosomal alignment (A) and separation (B) in latrunculin B. Either 30 or 100 nM latrunculin B was applied to zygotes 16–17 hours AF and samples of latrunculin-treated and controls were taken 4 hours later. Data points and bars are the means  $\pm$  s.d. of two experiments.

significantly different than controls ( $P \leq 0.001$ ; Fig. 4A). To determine whether the inhibition was due to a slowing of the alignment process in latrunculin B, olomoucine, which blocks the G2/M transition (Corellou et al., 2000), was added to extend the length of time zygotes spent in premetaphase. Premetaphase alignment in olomoucine was inhibited by latrunculin B when zygotes were examined at 25 or 40 hours AF ( $P \leq 0.0008$ ), indicating that the inhibition of alignment cannot be overcome by extending premetaphase. By contrast, postmetaphase alignment continued in the presence of latrunculin B; telophase arrays were approximately  $20^\circ$  better aligned than metaphase spindles in treated zygotes ( $P \leq 0.008$ ). In addition, the separation of the spindle poles that accompanies postmetaphase alignment also occurred in latrunculin B (Fig. 4B).

### Plasmolysis

Recently, plasmolysis has been shown to disrupt adhesions and spindle position in higher plants (Cleary, 2001) and we have previously shown that plasmolysis breaks adhesions in *P. compressa* zygotes (Henry et al., 1996). To determine the effects of plasmolysis on spindle alignments in *P. compressa* zygotes, germinated zygotes were transferred to hypertonic solutions. In ASW containing 0.6 or 0.7 M sucrose, plasmolysis was visually evident at the level of light microscopy; the plasma membrane pulled away from cell wall within the first few minutes after exposure. In ASW plus 0.6

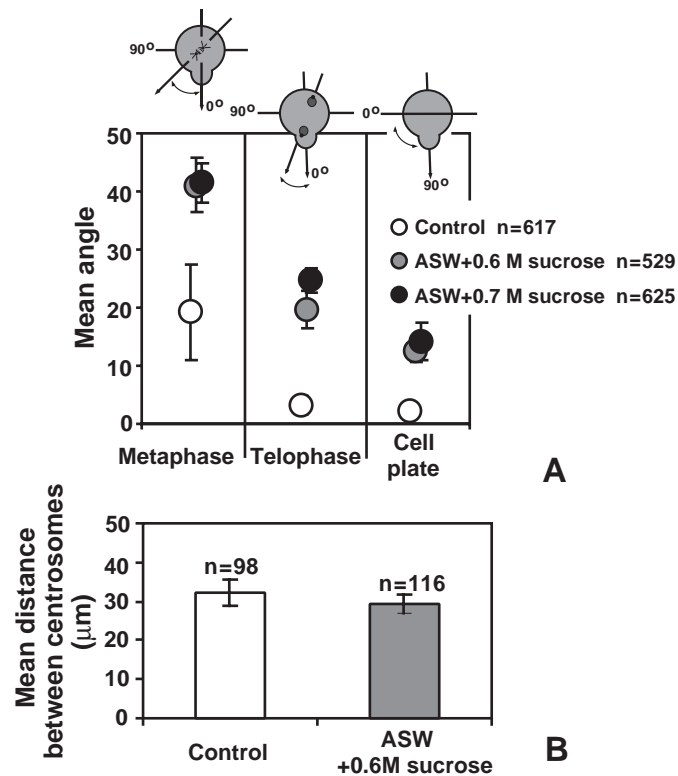


**Fig. 5.** Plasmolysis disrupts premetaphase alignment. Treated zygotes were transferred to ASW containing either 0.6 or 0.7 M sucrose at 15 hours AF. (A) Alignment angles. Data points are the means $\pm$ s.d. of three experiments. (B) The distance between the centrosomes at telophase; bars are the means $\pm$ s.d. of two experiments.

M sucrose separation of the membrane from the wall was detectable only in the rhizoid region whereas, in ASW plus 0.7 M sucrose, a gap between the membrane and the wall was visually evident in both the thallus and the rhizoid regions (not shown). Although development was slowed in the presence of 0.6 and 0.7 M sucrose, zygotes cultured in either solution did progress through mitosis and completed cytokinesis. (At higher concentrations of sucrose development was severely retarded.) The mean alignments in plasmolyzed zygotes at metaphase were greater than 40° (Fig. 5A), indicating that little to no premetaphase alignment had occurred. However, as was observed in latrunculin-treated zygotes, postmetaphase alignment proceeded in plasmolyzed zygotes; telophase arrays and cell plates were significantly better aligned than metaphase spindles ( $P \leq 0.003$ ). Separation of the mitotic spindle poles also occurred in plasmolyzed zygotes as the distance separating the two centrosomes at telophase was similar in zygotes cultured in ASW plus 0.6 M sucrose ( $29.3 \pm 2.5 \mu\text{m}$ ) and in controls ( $32.4 \pm 3.4 \mu\text{m}$ ) (Fig. 5B). Similar results were also found for zygotes incubated in ASW containing sorbitol (not shown).

#### Inhibition of secretion

Transmembrane linkages from the cell cortex to the wall contain secreted components (Henry et al., 1996), and we therefore investigated a possible role for secretion in centrosomal alignment. When Brefeldin A, a pharmacological agent that disrupts Golgi structure and thereby inhibits

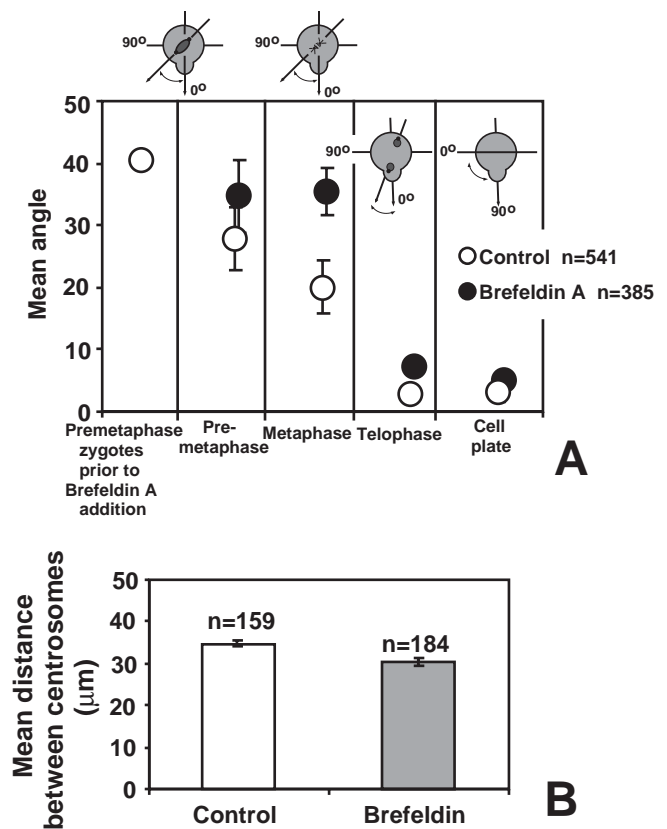


**Fig. 6.** Centrosomal alignment and separation in Brefeldin A.

(A) Centrosomal alignment angles were measured before transfer to Brefeldin A (at 15.5 hours AF) and again during mitosis (21.5 hours AF) on either untreated zygotes or on zygotes incubated in 5  $\mu\text{g/ml}$  Brefeldin A. Data points are the means $\pm$ s.d. of two experiments. (B) The distances between centrosomes at telophase were measured on zygotes cultured in 5  $\mu\text{g/ml}$  Brefeldin A from 9 hours AF and bars indicate the means $\pm$ s.d. of three experiments.

secretion in *P. compressa* (Hable and Kropf, 1998; Bisgrove and Kropf, 2001), was added to zygotes after germination, premetaphase alignment was disrupted, but postmetaphase alignment continued (Fig. 6A). In fact, the amount of postmetaphase alignment that occurred in Brefeldin A-treated zygotes ( $\sim 29^\circ$ ) was more than in controls ( $\sim 17^\circ$ ), suggesting that the majority of alignment can be completed after metaphase. By telophase, the centrosomal axes in treated zygotes were almost as well aligned as controls ( $7 \pm 0.3^\circ$  and  $3 \pm 0.3^\circ$ , respectively) and division plane alignments were similar in the two populations ( $5 \pm 0.4^\circ$  versus  $3 \pm 2^\circ$ ). Spindle poles also separated normally in Brefeldin A-treated zygotes (Fig. 6B).

#### Extracellular protease treatment

The role for transmembrane or extracellular proteins in centrosomal alignment was investigated by transferring germinated zygotes into ASW solutions containing the proteases thermolysin and proteinase K. Previous findings showed that treatment with these proteases significantly reduced the number of adhesions (Henry et al., 1996). Protease treatment inhibited premetaphase centrosomal alignment while postmetaphase alignment continued (Fig. 7A). As occurred

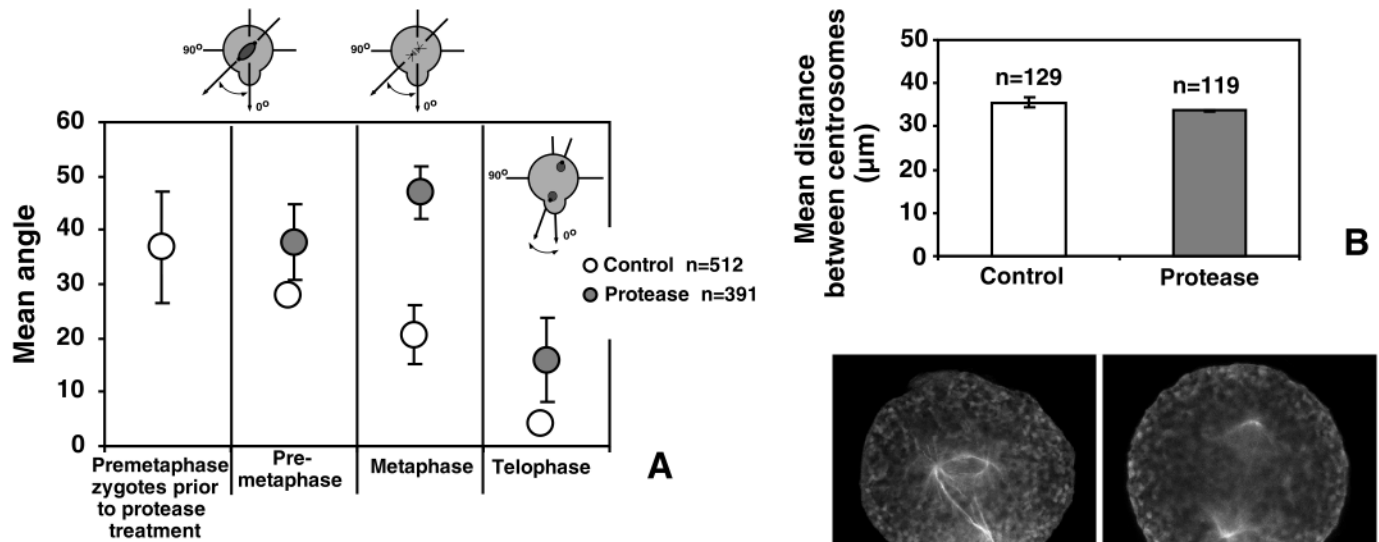


**Fig. 7.** Effects of externally applied proteases. Treated zygotes were incubated in 0.1% (w/v) thermolysin and 0.1% (w/v) proteinase K beginning 15–17 hours AF. (A) Centrosomal alignment angles were measured on zygotes prior to treatment and during mitosis. (B) Distances between centrosomes at telophase. Data points in A and bars in B are the means  $\pm$  s.d. of three experiments. Premetaphase (C) and telophase (D) microtubule arrays in protease-treated zygotes. Scale bar in C also applies to D.

in Brefeldin A, protease-treated zygotes actually underwent more postmetaphase alignment ( $\sim 31^\circ$ ) than controls ( $\sim 17^\circ$ ). Separation of the mitotic spindle poles continued in protease-treated zygotes (Fig. 7B) despite the fact that microtubule arrays were disrupted.

Following protease treatment, microtubules were fewer in number, shorter in length and did not extend into the cell cortex (Fig. 7C,D). In addition, the intensity of microtubule staining appeared reduced. The disruption of microtubule arrays was apparent within 1 hour of treatment and did not change with time or with addition of fresh proteases (data not shown). The effect of external proteases on microtubule arrays implicates transmembrane and/or extracellular proteins in microtubule stability. However, it should be noted that none of the other treatments that disrupt adhesions had any noticeable effect on microtubule arrays (data not shown).

### Inhibition of polysaccharide deposition

To determine whether cell wall polysaccharides were involved in centrosomal alignment, treatments that compromised polysaccharide deposition into the wall were examined. Cell walls of fucoid algae contain proteins, cellulose, fucans, polyphenols and alginic acid (Quatrano and Stevens, 1976; Schoenwaelder and Wiencke, 2000). The deposition of cellulose, a polysaccharide that is synthesized in situ by a cellulose synthase complex in the plasma membrane of the zygote (Peng and Jaffe, 1976), was inhibited by incubating zygotes in isoxaben beginning 1 hour AF. Although *P. compressa* zygotes cultured in isoxaben develop weak cell walls that are compromised for cellulose (Bisgrove and Kropf, 2001), isoxaben appeared to have no effect on centrosomal alignment (Fig. 8A). To inhibit the deposition of sulfated wall components, such as the fucan F2 and polyphenolics, zygotes were cultured in ASW lacking added sulfate beginning 1 hour AF (Brawley and Quatrano, 1979). These zygotes deposit

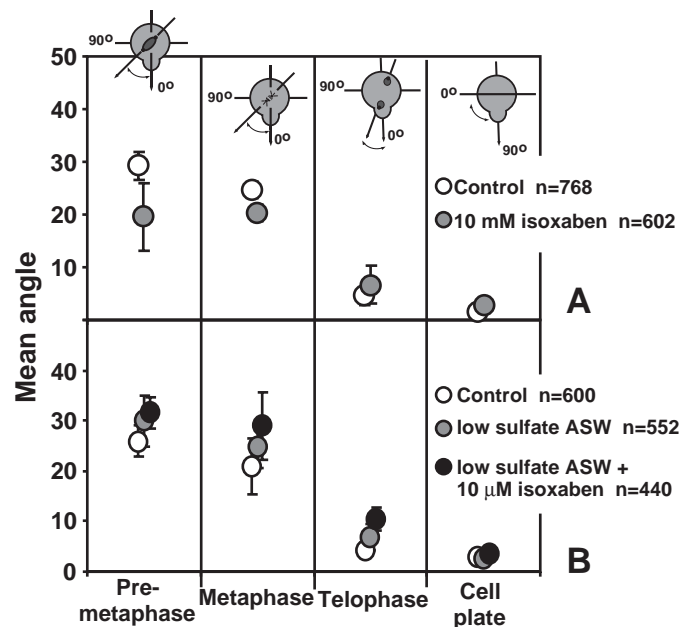


**Fig. 8.** Inhibition of cell wall deposition. Zygotes were transferred to ASW containing isoxaben and/or low sulfate ASW at 0–1 hours AF. (A) Centrosomal alignments in 10  $\mu$ M isoxaben; (B) low sulfate ASW  $\pm$  10  $\mu$ M isoxaben. Data points are the means  $\pm$  s.d. of three experiments.

disorganized and weakened walls at the rhizoid apex (Bisgrove and Kropf, 2001) but, as was seen with isoxaben, there was no effect on centrosomal alignments (Fig. 8B). Pre- and postmetaphase alignments were as good as controls even when zygotes were cultured in both isoxaben and low sulfate ASW (Fig. 8B). These findings indicate that alignment can occur in zygotes with compromised walls.

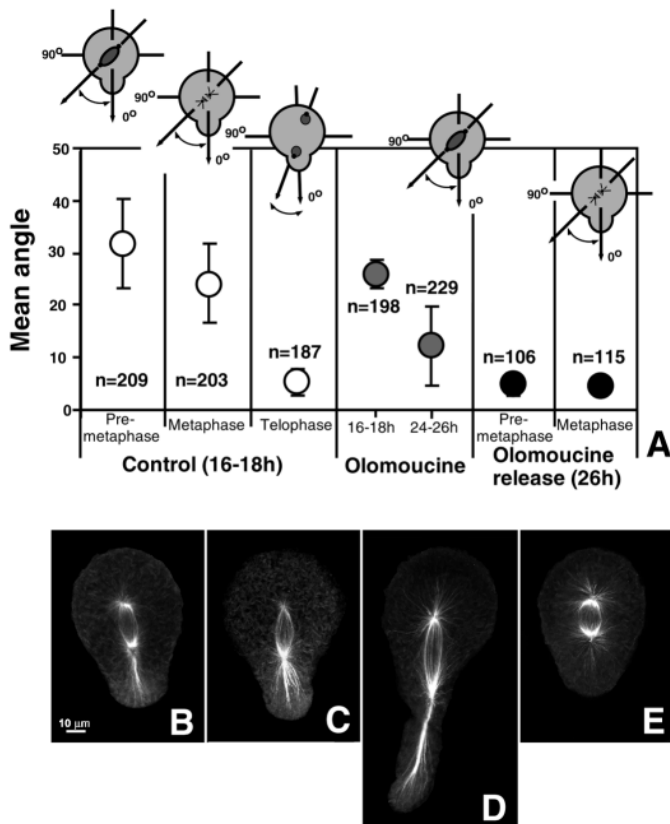


**Fig. 9.** Centrosomal alignment in olomoucine. (A) Alignment angles were measured on four populations of either untreated zygotes progressing through mitosis or zygotes incubated in 35  $\mu$ M olomoucine beginning 5 hours AF. In two of the populations, zygotes were released from olomoucine 24 hours AF and alignments of the centrosomal axes were measured on premetaphase and metaphase zygotes. Data points are means $\pm$ s.d. (B) An elongated nucleus in an untreated zygote 16 hours AF. (C,D) Nuclei in olomoucine-treated zygotes 25.5 hours AF are also elongated. (E) An oval nucleus in a zygote cultured in olomoucine from 5 to 15.5 hours AF and then olomoucine and 30 nM latrunculin B from 15.5 hours AF until 39.5 hours AF. Scale bar in B also applies to C-E.

### Centrosomal alignment in the absence of spindle formation

Data presented above indicate that additional alignment in postmetaphase can compensate for inhibition of premetaphase alignment (compare Fig. 6 and Fig. 7). Conversely, to determine whether the majority of alignment could be accomplished prior to metaphase, zygotes were cultured in olomoucine, a competitive inhibitor of cyclin-dependent kinases in plant and animal cells (Abraham et al., 1995). When olomoucine is added during S phase (5 hours AF), fucoid zygotes germinate but the cell cycle is blocked at the G2/M transition and zygotes do not enter mitosis (Corellou et al., 2000). We compared centrosomal alignments from zygotes cultured continuously from 5 hours AF in olomoucine with alignments in untreated zygotes at different stages of development (Fig. 9). The mean alignment of the centrosomal axes in olomoucine-treated zygotes sampled 16–18 hours AF was  $26\pm 3^\circ$ , similar to the alignments of metaphase spindles in untreated zygotes of the same age ( $24\pm 7^\circ$ ). Alignment

continued in olomoucine and by 24–26 hours AF the mean alignment angle was  $12\pm 8^\circ$ , nearly as good as telophase alignment in untreated zygotes ( $5\pm 3^\circ$ ). Thus, entry into metaphase was not required for continued alignment.

The two olomoucine-cultured populations that were the best aligned at 24 hours AF were released from the drug and subsequent development was analyzed. Both populations entered mitosis rapidly and within 2 hours some of the zygotes formed metaphase spindles. The metaphase spindle alignments in these populations were  $5\pm 2^\circ$ , identical to premetaphase alignments measured in treated zygotes at the time of release. These findings suggest that, despite the lack of microtubule contacts with the cell cortex, metaphase spindles do not drift out of alignment.

Untreated premetaphase zygotes with well aligned centrosomal axes had oval nuclei that were elongated, as if stretched between the rhizoid and thallus poles (Fig. 9B). Nuclei were also elongated along the growth axis in all olomoucine-treated zygotes (Fig. 9C) and in some zygotes the lengthening of the nucleus was extreme (Fig. 9D). This was often the case in zygotes that developed long rhizoids; even in these zygotes, densely packed microtubules extended all the way to the cell cortex at the rhizoid tip. F-actin depolymerization by treatment with latrunculin B inhibited nuclear elongation; nuclei in zygotes cultured in latrunculin B alone (not shown) or in both olomoucine and latrunculin B (Fig. 9E) remained round to oval and never took on a stretched appearance. These observations indicate that the elongation of the nucleus is F-actin dependent, and suggest that the centrosomes may be pulled toward opposite poles during premetaphase alignment.

### DISCUSSION

We previously reported that centrosomal alignment occurs by a nuclear rotation that orients the centrosomal axis parallel with the rhizoid/thallus growth axis (Allen and Kropf, 1992; Bisgrove and Kropf, 1998). In this report we find that this premetaphase rotation only crudely aligns the centrosomal axis with the growth axis, and therefore metaphase spindles are often skewed. Little to no alignment occurs during metaphase, but alignment resumes thereafter and by late telophase the centrosomal axes are as well aligned as the cell plates that subsequently form. Spindle alignment in budding *Saccharomyces cerevisiae* occurs by a similar two-step process in which there is a crude alignment with the mother-bud axis prior to metaphase followed by more precise alignment during anaphase spindle elongation (Shaw et al., 1997).

Both pre- and postmetaphase alignments correlate temporally with microtubule arrays that extend into the cellular cortex. (However, it should be noted that cortical microtubules might also be present at metaphase but not preserved well during fixation.) Despite this correlation, the two phases of alignment apparently occur by different mechanisms. Several treatments that disrupt cortical adhesions inhibited premetaphase alignment but had little or no effect on either postmetaphase alignment or separation of the spindle poles. These findings necessitate a revision of previously published models; we now propose that premetaphase alignment occurs by a nuclear rotation involving cortical adhesions and that

postmetaphase alignment is linked to the elongation of the mitotic apparatus in anaphase/telophase by a mechanism that is as yet poorly understood.

### Premetaphase centrosomal alignment

Our current findings provide the first evidence that physical links from the cellular cortex to the cell wall are important in centrosomal alignment. Premetaphase alignment was inhibited by F-actin depolymerization, plasmolysis, protease treatment or inhibition of secretion, and the first three treatments have also been shown to reduce the number of, or to sever, adhesions in fucoid zygotes (Henry et al., 1996). The data are consistent with adhesions composed of cortical F-actin linked to proteins deposited by the secretory pathway into the plasma membrane and/or cell wall. Other wall components, specifically cellulose and/or sulfated wall components (F2 fucans and polyphenols), appear not to be integral components of adhesions involved in premetaphase alignments. Astral microtubules also function in premetaphase alignment because treatments with low doses of oryzalin or paclitaxel are inhibitory.

These findings support a model in which microtubules extending from the perinuclear centrosomes are captured by cortical adhesions that are located throughout the cell cortex but are more concentrated in the rhizoid apex (Henry et al., 1996). Microtubule capture may involve the actin component of the adhesion (Schuyler and Pellman, 2001). Once captured, the microtubules exert a pulling force that moves the associated centrosome toward the cortex. Stochastically, one centrosome resides closer to the rhizoid apex and therefore anchors more microtubules in the rhizoid cortex. This centrosome is pulled towards the rhizoid apex while the other centrosome is either held in the middle of the cell or pulled toward the thallus, possibly by microtubule interactions with adhesions in the thallus cortex. A similar microtubule-based search and capture mechanism is thought to align the spindle during asymmetric divisions in budding yeast and in *Caenorhabditis elegans* zygotes. In budding yeast, dynamic microtubules emanating from the spindle pole body are transiently captured when they interact with the bud cell cortex, and pulling forces bring the spindle pole body and associated nucleus into the mother-bud neck (Shaw et al., 1997; Carminati and Stearns, 1997). Recently, some of the molecules involved in microtubule capture have been identified; these include Bim1p and Kar9p (Schuyler and Pellman, 2001). Two types of pulling forces are exerted during yeast spindle alignment; capture of free microtubule ends followed by microtubule depolymerization and dynein-dependent microtubule sliding along the cell cortex (Adames and Cooper, 2000). In premetaphase *P. compressa* zygotes, the presence of microtubules that terminate end-on at the surface and microtubules that curve along the cell cortex suggests that both microtubule depolymerization and sliding may contribute to rotational alignment of the nucleus.

The distortion of nuclear morphology in *P. compressa* supports the notion that centrosomes are pulled, rather than pushed, into alignment. Nuclei undergoing alignment appear stretched between the rhizoid and thallus poles and this nuclear asymmetry intensifies as alignment progresses. Treatment with latrunculin B prevents both nuclear stretching and rotational alignment, consistent with force generation by microtubules anchored at cortical adhesions containing F-actin. However,

the cell wall need not be structurally intact for ample force generation since inhibiting the deposition of cellulose or sulfated components significantly weakens the wall (Bisgrove and Kropf, 2001), but has no effect on premetaphase alignment. Recently F-actin at cortical adhesions has also been shown to be involved in spindle position in plant cells (Cleary, 2001).

### Postmetaphase alignment

Our data for the second phase of centrosomal alignment are not consistent with a model in which pulling forces are exerted on centrosomal microtubules anchored at cortical adhesions. Instead, postmetaphase alignment appears to be associated with elongation of the mitotic apparatus during anaphase B and early telophase. Since none of the treatments affected postmetaphase alignment, we can only speculate as to its mechanism. One possibility is that centrosomal centering mechanisms acting during spindle elongation contribute to alignment. Centrosomal centering involves interactions between centrosomal microtubules and fixed objects such as the cell cortex (Reinsch and Gonczy, 1998). Centrosomes may be pushed away from the cortex by polymerizing microtubules that impact the cortex or, alternatively, they may be pulled towards the cortex by cytoplasmic motors (Hill and Kirschner, 1982; Bjercknes, 1986; Holy et al., 1997; Reinsch and Gonczy, 1998). In principle, in a cell that is longer than it is wide (such as the *P. compressa* zygote) centrosomal centering forces acting on the two spindle poles as they separate could align the two poles parallel to the long axis of the cell if the two spindle poles move as a unit (Bjercknes, 1986). There is evidence that cell morphology can affect spindle positions within dividing cells, in particular plant cells (Oud and Nanninga, 1992; Palevitz, 1993; de Ruijter et al., 1997).

If such a mechanism were operating in *P. compressa*, postmetaphase alignment would be expected to be sensitive to microtubule disruption. Instead, we found that postmetaphase alignment was not sensitive to partial microtubule depolymerization (oryzalin or protease treatment) or stabilization (paclitaxel treatment). However, the microtubules remaining following these treatments were sufficient to elongate the spindle, and may be capable of interacting with the surface to complete alignment. Higher drug doses block mitosis (Corellou et al., 2000) and therefore could not be examined.

In animal cells, spindle orientation determines the subsequent plane of division by a mechanism that appears to involve unknown signals from the spindle midzone to the cell cortex (Hales et al., 1999). In other cell types (for example, plant cells, *S. cerevisiae* and *Schizosaccharomyces pombe*), the division plane is specified prior to mitosis (Hales et al., 1999). How and when the plane of cytokinesis is determined in fucoid algae is unknown. Our findings indicate that if the mitotic apparatus positions the cell plate in fucoid zygotes, it must do so late in telophase rather than during anaphase as it does in animal cells. We are currently investigating whether the mitotic apparatus specifies division plane or, alternatively, the mitotic apparatus is brought into alignment with a predetermined division site.

We thank Stephen Ruth for measuring alignments on plasmolyzed zygotes, Francois-Yves Bouget for his gift of olomoucine, I. Larrinua

for his gift of isoxaben, and Whitney Hable for critical discussions. This research was supported by NSF award IBN 9807811 to D.L.K. and a NSERC postdoctoral fellowship PDF-219981-1999 awarded to S.R.B.

## REFERENCES

- Abraham, R. T., Acquarone, M., Andersen, A., Asensi, A., Belle, R., Berger, F., Bergounioux, C., Brunn, G., Buquet-Fagot, C., Fagot, D. et al. (1995). Cellular effects of olomoucine, an inhibitor of cyclin-dependent kinases. *Biol. Cell* **83**, 105-120.
- Adames, N. R. and Cooper, J. A. (2000). Microtubule interactions with the cell cortex causing nuclear movements in *Saccharomyces cerevisiae*. *J. Cell Biol.* **149**, 863-874.
- Alessa, L. and Kropf, D. L. (1999). F-actin marks the rhizoid pole in living *Pelvetia compressa* zygotes. *Development* **126**, 201-209.
- Allen, V. W. and Kropf, D. L. (1992). Nuclear rotation and lineage specification in *Pelvetia* embryos. *Development* **115**, 873-883.
- Bachewich, C. L. and Heath, I. B. (1997). Differential cytoplasm-plasma membrane-cell wall adhesion patterns and their relationships to hyphal tip growth and organelle motility. *Protoplasma* **200**, 71-86.
- Bisgrove, S. R. and Kropf, D. L. (1998). Alignment of centrosomal and growth axes is a late event during polarization of *Pelvetia compressa* zygotes. *Dev. Biol.* **194**, 246-256.
- Bisgrove, S. R. and Kropf, D. L. (2001). Cell wall deposition during morphogenesis in fucoid algae. *Planta* **212**, 648-658.
- Bjerknes, M. (1986). Physical theory of the orientation of astral mitotic spindles. *Science* **234**, 1413-1416.
- Brawley, S. H. and Quatrano, R. S. (1979). Sulfation of fucoidin in *Fucus* embryos. IV. Autoradiographic investigations of fucoidin sulfation and secretion during differentiation and the effect of cytochalasin treatment. *Dev. Biol.* **73**, 193-205.
- Carminati, J. L. and Stearns, T. (1997). Microtubules orient the mitotic spindle in yeast through dynein-dependent interactions with the cell cortex. *J. Cell Biol.* **138**, 629-641.
- Cleary, A. L. (2001). Plasma membrane-cell wall connections: roles in mitosis and cytokinesis revealed by plasmolysis of *Tradescantia virginiana* leaf epidermal cells. *Protoplasma* **215**, 21-34.
- Corellou, F. C., Bisgrove, S. R., Kropf, D. L., Meijer, L., Kloareg, B. and Bouget, F.-Y. (2000). A S/M DNA replication checkpoint prevents nuclear and cytoplasmic events of cell division including centrosomal axis alignment and inhibits activation of cyclin dependent kinase-like proteins in fucoid zygotes. *Development* **127**, 1651-1660.
- de Ruijter, N. C. A., Pietrusiewicz, J., Montijn, M. B., Schel, J. H. N. and Van Lammeren, A. A. M. (1997). Spatial limitations induce spindle tilting and result in oblique phragmoplasts in *Vicia faba* L. root tip cells, but do not result in oblique cell walls. *Acta. Bot. Neerl.* **46**, 279-290.
- Fowler, J. E. and Quatrano, R. S. (1997). Plant cell morphogenesis: Plasma membrane interactions with the cytoskeleton and cell wall. *Annu. Rev. Cell Dev. Biol.* **13**, 697-743.
- Hable, W. and Kropf, D. L. (1998). Roles of secretion and the cytoskeleton in cell adhesion and polarity establishment in *Pelvetia compressa* zygotes. *Dev. Biol.* **198**, 45-56.
- Hales, K. G., Bi, E., Wu, J., Adam, J. C., Yu, I. and Pringle, J. R. (1999). Cytokinesis: an emerging unified theory for eukaryotes? *Curr. Opin. Cell Biol.* **11**, 717-725.
- Hawkins, N. and Garriga, G. (1998). Asymmetric cell division: from A to Z. *Genes Dev.* **12**, 3625.
- Henry, C. A., Jordan, J. R. and Kropf, D. L. (1996). Localized membrane-wall adhesions in *Pelvetia* zygotes. *Protoplasma* **190**, 39-52.
- Hill, T. L. and Kirschner, M. W. (1982). Bioenergetics and kinetics of microtubule and actin filament assembly-disassembly. *Int. Rev. Cytol.* **78**, 1-125.
- Holy, T. E., Dogterom, M., Yurke, B. and Leibler, S. (1997). Assembly and positioning of microtubule asters in microfabricated chambers. *Proc. Natl. Acad. Sci. USA* **94**, 6228-6231.
- Kagawa, T., Kadota, A. and Wada, M. (1992). The junction between the plasma membrane and the cell wall in fern protonemal cells, as visualized after plasmolysis, and its dependence on arrays of cortical microtubules. *Protoplasma* **170**, 186-190.
- Kaminskyj, S. G. W. and Heath, I. B. (1995). Integrin and spectrin homologues and cytoplasm-wall adhesion in tip growth. *J. Cell Sci.* **108**, 849-856.
- Kirk, M. M., Ransick, A., McRae, S. E. and Kirk, D. L. (1993). The relationship between cell size and cell fate in *Volvox carteri*. *J. Cell Biol.* **123**, 191-208.
- Kohorn, B. D. (2000). Plasma membrane-cell wall contacts. *Plant Physiol.* **124**, 31-38.
- Kropf, D. L. (1997). Induction of polarity in fucoid zygotes. *Plant Cell* **9**, 1011-1020.
- Kropf, D. L., Bisgrove, S. R. and Hable, W. E. (1999). Establishing a growth axis in fucoid algae. *Trends Plant Sci.* **4**, 490-494.
- Mellersh, D. G. and Heath, M. C. (2001). Plasma membrane-cell wall adhesion is required for expression of plant defense responses during fungal penetration. *Plant Cell* **13**, 413-424.
- Oud, J. L. and Nanninga, N. (1992). Cell shape, chromosome orientation and the position of the plane of division in *Vicia faba* root cortex cells. *J. Cell Sci.* **103**, 847-855.
- Palevitz, B. A. (1993). Morphological plasticity of the mitotic apparatus in plants and its developmental consequences. *Plant Cell* **5**, 1001-1009.
- Peng, H. B. and Jaffe, L. F. (1976). Cell-wall formation in *Pelvetia* embryos. A freeze-fracture study. *Planta* **133**, 57-71.
- Quatrano, R. S. and Stevens, P. T. (1976). Cell wall assembly in *Fucus* zygotes. I. Characterization of the polysaccharide components. *Plant Physiol.* **58**, 224-231.
- Reinsch, S. and Gonczy, P. (1998). Mechanisms of nuclear positioning. *J. Cell Sci.* **111**, 2283-2295.
- Rose, L. S. and Kempthues, K. J. (1998). Early patterning of the *C. elegans* embryo. *Annu. Rev. Genet.* **32**, 521-545.
- Schoenwaelder, M. E. A. and Wiencke, C. (2000). Phenolic compounds in embryos during development of several northern hemisphere fucoids. *Plant Biol.* **2**, 24-33.
- Schuyler, S. C. and Pellman, D. (2001). Search capture and signal: games microtubules and centrosomes play. *J. Cell Sci.* **114**, 247-255.
- Serrao, E. A., Alice, L. A. and Brawley, S. H. (1999). Evolution of the Fucaaceae (Phaeophyceae) inferred from nrDNA-ITS. *J. Phycol.* **35**, 382-394.
- Shaw, S. L., Yeh, E., Maddox, P., Salmon, E. D. and Bloom, K. (1997). Astral microtubule dynamics in yeast: A microtubule-based searching mechanism for spindle orientation and nuclear migration into the bud. *J. Cell Biol.* **139**, 985-994.